bioRxiv preprint doi: https://doi.org/10.1101/2022.11.26.518005; this version posted November 30, 2022. The copyright holder for this preprint (which was not certified by peer review) is the author/funder, who has granted bioRxiv a license to display the preprint in perpetuity. It is made available under aCC-BY-NC-ND 4.0 International license.

1 2 # An Optimized Circular Polymerase Extension Reaction-based Method for Functional Analysis of SARS-CoV-2

3

4 GuanQun Liu* and Michaela U. Gack*

5 Florida Research and Innovation Center, Cleveland Clinic, Port St. Lucie, Florida, USA

6

7 *Correspondence: LIUG2@ccf.org (G.L.); gackm@ccf.org (M.U.G.)

8

9

10 ## SUMMARY

11 Reverse genetics systems have been crucial for studying specific viral genes and their
12 relevance in the virus lifecycle, and become important tools for the rational attenuation of
13 viruses and thereby for vaccine design. Recent rapid progress has been made in the
14 establishment of reverse genetics systems for functional analysis of SARS-CoV-2, a
15 coronavirus that causes the ongoing COVID-19 pandemic that has resulted in detrimental public
16 health and economic burden. Among the different reverse genetics approaches, CPER (circular
17 polymerase extension reaction) has become one of the leading methodologies to generate
18 recombinant SARS-CoV-2 infectious clones due to its accuracy, efficiency, and flexibility. Here,
19 we report an optimized CPER methodology which, through the use of a modified linker plasmid
20 and by performing DNA nick ligation and direct transfection of permissive cells, overcomes
21 certain intrinsic limitations of the 'traditional' CPER approaches for SARS-CoV-2, allowing for
22 efficient virus rescue. This optimized CPER system may facilitate research studies to assess the
23 contribution of SARS-CoV-2 genes and individual motifs or residues to virus replication,
24 pathogenesis and immune escape, and may also be adapted to other viruses.

bioRxiv preprint doi: https://doi.org/10.1101/2022.11.26.518005; this version posted November 30, 2022. The copyright holder for this preprint (which was not certified by peer review) is the author/funder, who has granted bioRxiv a license to display the preprint in perpetuity. It is made available under aCC-BY-NC-ND 4.0 International license.

25 **INTRODUCTION**

26 Functional analysis of individual viral genes including embedded motifs and individual
27 residues has been essential for understanding key functions of viruses such as viral entry,
28 genome amplification, or escape from innate or adaptive immunity. Key to these studies has
29 been the establishment of viral reverse genetics systems, which allow investigation of viral gene
30 functions through mutagenesis [1, 2]. In addition, reverse genetics approaches for generating
31 mutant recombinant viruses have become important for the rational design of replication-
32 impaired, so-called "live-attenuated" viruses, which may represent vaccine candidates.
33 Moreover, reverse genetics technologies enable studying viral evasion of antibody responses
34 (*e.g.* by the coronaviral spike protein) and thereby aid in mRNA vaccine design [3]. Therefore,
35 the development of efficient and accurate methodologies for generating viral infectious clones
36 including recombinant mutant viruses has not only become an integral component of
37 fundamental virology research, but also has great value for translational research and the
38 design of novel vaccines [4].

39 SARS-CoV-2, a member of the large family of *Coronaviridae*, emerged in Wuhan, China,
40 in late 2019 and then spread rapidly across the globe where it has caused substantial morbidity
41 and mortality as well as severe economic losses [5]. SARS-CoV-2 is one of the largest RNA
42 viruses. Its positive-sense genome is ~30 kb long and comprises a defined organization that
43 encodes for ~30 gene products or proteins [6]. Since the emergence of SARS-CoV-2, rapid
44 progress has been made in understanding how individual viral proteins or enzymes (*e.g.* spike
45 protein or the RNA-dependent RNA polymerase) fulfill key functions in the viral lifecycle such as
46 mediating virus entry and immune evasion or genome amplification. Studies to characterize viral
47 proteins in isolation – either through ectopic expression in mammalian cells or by *in vitro*
48 analysis following protein purification – have tremendously enhanced our understanding of how
49 SARS-CoV-2 proteins function and provided important insight into their catalytic activities or

bioRxiv preprint doi: https://doi.org/10.1101/2022.11.26.518005; this version posted November 30, 2022. The copyright holder for this preprint (which was not certified by peer review) is the author/funder, who has granted bioRxiv a license to display the preprint in perpetuity. It is made available under aCC-BY-NC-ND 4.0 International license.

50 interactions with host-cell factors or other viral proteins. However, the engineering of mutant
51 recombinant viruses in which specific genes/residues are deleted or mutated has been essential
52 for determining how relevant individual genes or specific motifs/residues are for virus infection,
53 pathogenesis or immune evasion. The large genome size of SARS-CoV-2 has hampered the
54 development of plasmid-based reverse genetics systems for this virus (and also other
55 coronaviruses) that have been used for many other RNA viruses (*i.e.* influenza and flaviviruses)
56 [4]. Therefore, bacterial artificial chromosome (BAC)-based technologies (typically used for
57 mutagenesis of large DNA viruses such as herpesviruses), *in vitro* cDNA fragment ligation, and
58 yeast-based synthetic biology approaches have been traditionally used for generating
59 recombinant coronaviruses including SARS-CoV-2 [7-15].

60 In 2021, the adaptation of a circular polymerase extension reaction (CPER)-based
61 approach, which has been successfully used for construction of flavivirus infectious clones [16],
62 was reported for the generation of recombinant SARS-CoV-2 [17, 18]. Advantages of the CPER
63 method include high-fidelity preservation of viral genome sequences with minimal or no
64 unwanted mutations, as compared to the BAC and *in vitro* ligation methodologies which can
65 introduce inexplicable insertions or deletions during bacterial propagation steps. Additionally,
66 CPER allows for flexibility in viral sequence manipulation by PCR-based mutagenesis, while the
67 BAC methodology relies on *de novo* assembly or homologous recombination in special bacterial
68 systems. Furthermore, the straightforward and streamlined workflow of CPER allows for
69 infectious clone construction in a single-tube reaction, which is in sharp contrast to BAC cloning
70 and *in vitro* ligation of cDNA fragments that require cumbersome procedures and complex
71 experimental techniques.

72 Integral to the CPER technology is PCR-based amplification of cDNA fragments that
73 cover the complete viral genome (30 kb in the case of SARS-CoV-2) and carry overlapping
74 sequences. With the use of a 'linker' fragment that connects the viral 5' and 3' untranslated

bioRxiv preprint doi: https://doi.org/10.1101/2022.11.26.518005; this version posted November 30, 2022. The copyright holder for this preprint (which was not certified by peer review) is the author/funder, who has granted bioRxiv a license to display the preprint in perpetuity. It is made available under aCC-BY-NC-ND 4.0 International license.

75 regions (UTRs) with functional mammalian transcription initiation and termination elements, the
76 individual cDNA fragments are extended in a single PCR reaction to assemble into a
77 circularized full-length viral cDNA clone. The circularized cDNA clone is then delivered (typically
78 by transfection) into mammalian cells, leading to the intracellular synthesis of viral genomic RNA
79 and, ultimately, the production of infectious virus. Although the CPER platform has already
80 greatly facilitated studies to functionally characterize SARS-CoV-2 genes and specific
81 mutations, some intrinsic limitations still exist that hamper the robustness and efficiency of virus
82 rescue.

83 Here, we report an optimized CPER methodology for reverse genetics engineering of
84 SARS-CoV-2. Specifically, we utilized a modified linker plasmid, added a new step of ligating
85 DNA nicks, and also applied direct transfection of the circularized infectious cDNA clone into
86 highly permissive cells, which resulted in more rapid rescue of the virus and efficient viral yields.

87

88 **RESULTS**

89 **Optimization of the CPER approach for efficient SARS-CoV-2 rescue**

90 The CPER method builds principally on overlap extension PCR that fuses several
91 double-stranded DNA (dsDNA) fragments containing 20- to 50-bp homologous ends into one
92 large fragment [19]. Compared to the traditional overlap extension PCR, which uses a set of two
93 distal primers to facilitate the generation of the combined fragment, CPER does not amplify
94 fragments using such primers but instead utilizes an additional fragment that overlaps with the
95 first and the last fragment to be joined, thereby circularizing the self-primed and extended
96 dsDNA product. In CPER-based bacterial cloning, this additional fragment is typically a
97 linearized plasmid vector generated by restriction digestion or PCR. As a result, the CPER
98 product resembles a relaxed circular plasmid with staggered nicks which locate to the 5' end of

bioRxiv preprint doi: https://doi.org/10.1101/2022.11.26.518005; this version posted November 30, 2022. The copyright holder for this preprint (which was not certified by peer review) is the author/funder, who has granted bioRxiv a license to display the preprint in perpetuity. It is made available under aCC-BY-NC-ND 4.0 International license.

99 each strand of the individual fragment following the respective 'round-the-horn' amplification, as
100 commonly seen in the QuikChange® approach of site-directed mutagenesis [20].

101 Adaptation of the CPER approach to *de novo* assembly of infectious clones for positive-
102 strand RNA viruses is primarily achieved by substituting a linker fragment for the linearized
103 vector used in CPER-mediated plasmid cloning. The design of the linker fragment draws
104 inspiration from plasmid-launched mRNA synthesis driven by the mammalian RNA polymerase
105 II (Pol II) promoter, as the genomes of several positive-sense RNA viruses including flaviviruses
106 and coronaviruses contain a 5' cap structure like cellular mRNAs and undergo cap-dependent
107 translation. In addition to the Pol II promoter, the linker fragment also contains a polyadenylation
108 signal for transcription termination and, importantly, a self-cleaving ribozyme sequence in front
109 of the poly(A) signal to ensure accurate processing of the 3' end of the RNA transcript to match
110 the authentic viral genome sequence. Notably, while the linker fragment is usually cloned into a
111 plasmid for long-term maintenance in *E. coli*, only the portion containing the mammalian
112 transcription elements, but not the bacterial propagation cassettes, is amplified and used in
113 CPER assembly.

114 Despite the successful adaptation of the CPER technology for the generation of
115 infectious clones, CPER has a major intrinsic limitation, which is the presence of staggered
116 nicks that impede efficient expression in mammalian cells. Whereas nicked plasmids are known
117 to be seamlessly repaired upon transformation into *E. coli*, the precise fate of a circularized,
118 nick-containing dsDNA inside a mammalian cell remains elusive. The presence of nicks in the
119 template strand can cause Pol II pausing and likely also template misalignment, which may
120 eventually lead to unwanted mutations [21]. In CPER-derived infectious clones, the circular
121 template strand extended from each fragment contains a nick, which, depending on the genome
122 segmentation scheme used for assembly, locates to different coding or noncoding regions of the
123 viral genome. Although the sequence contexts in which the nicks situate may permit Pol II

bioRxiv preprint doi: https://doi.org/10.1101/2022.11.26.518005; this version posted November 30, 2022. The copyright holder for this preprint (which was not certified by peer review) is the author/funder, who has granted bioRxiv a license to display the preprint in perpetuity. It is made available under aCC-BY-NC-ND 4.0 International license.

124 bypassing, how the template discontinuity affects the overall Pol II transcription efficiency, and
125 hence the synthesis of full-length viral genomes, in mammalian cells remains unclear.

126 Another limitation of the current CPER approaches for SARS-CoV-2 rescue lies in the
127 choice of cell lines for transfection of the CPER product [17, 18]. While HEK293-derived cell
128 lines have been successfully used for reverse genetics systems for a variety of viruses from
129 diverse families due to their robust transfectability, the use of HEK293 cells for SARS-CoV-2
130 rescue can be less efficient because of the unique cellular tropism of the virus and the critical
131 host factors required for virus entry and replication. To date, three mammalian cell lines are
132 commonly used for *in vitro* propagation of SARS-CoV-2 to high titers. These include Vero E6
133 (African green monkey kidney epithelial), Caco-2 (human colonic epithelial), and Calu-3 (human
134 lung epithelial) cells. All three cell lines express the receptor for SARS-CoV-2, angiotensin-
135 converting enzyme 2 (ACE2), while the latter two express also transmembrane serine protease
136 2 (TMPRSS2), a critical early entry cofactor [22]. In addition to priming direct cell membrane
137 fusion, the presence of TMPRSS2 safeguards the integrity of the polybasic furin cleavage site in
138 the viral spike gene, which is selectively deleted during serial passaging in Vero E6 cells due to
139 viral host adaptation [23]. To this end, Vero E6 cells stably expressing human TMPRSS2 (Vero
140 E6-TMPRSS2) have been widely used for the propagation of ancestral and emerging SARS-
141 CoV-2 strains including the variants of concern (VOCs). More importantly, given the nature that
142 Vero cells lack interferon (IFN) production [24], it remains the first-line cell system for generating
143 and propagating recombinant mutant viruses that are attenuated through selective ablation of
144 viral gene functions that evade or antagonize IFN-mediated antiviral innate immunity (*e.g.*
145 SARS-CoV-2 papain-like protease (PLpro) which is an IFN antagonist [25, 26]).

146 Taking these limitations into account, we rationally optimized CPER for SARS-CoV-2 by
147 adding new steps to seal the nicks in the CPER product and by using a modified linker plasmid
148 as well as a different cell line for transfection of the CPER product (**Figure 1A**). Specifically,

bioRxiv preprint doi: https://doi.org/10.1101/2022.11.26.518005; this version posted November 30, 2022. The copyright holder for this preprint (which was not certified by peer review) is the author/funder, who has granted bioRxiv a license to display the preprint in perpetuity. It is made available under aCC-BY-NC-ND 4.0 International license.

149 under the same genome segmentation scheme reported by Torii *et al.* [18], gel-purified viral
150 cDNA fragments were phosphorylated at the 5' end by using a T4 polynucleotide kinase. Equal
151 molar amounts of the phosphorylated fragments were then subjected to CPER assembly using
152 the cycling 'condition 3' as described previously [18]. Immediately before transfection, the nicks
153 in the CPER product were sealed by using a high-fidelity and thermostable Taq DNA ligase that
154 joins the extended 3'–OH terminus with its originating 5'–phosphorylated terminus, giving rise to
155 a closed circular cDNA infectious clone. Then, the sealed CPER product was directly
156 transfected into a monolayer of Vero E6-TMPRSS2 cells by using the *Trans*IT-X2 dynamic
157 delivery system (**Figure 1A**). Furthermore, to ensure efficient Pol II termination and to prevent
158 Pol II read-through in the linker region, which may confound ribozyme processing at the
159 transcript 3' end or interfere with new transcription initiation, we also replaced the 'spacer'
160 sequence that is located between the poly(A) signal and CMV enhancer/promoter with a
161 functional Pol II transcriptional pause signal from the human α2 globin gene known to minimize
162 promoter crosstalk [27]. The resultant linker sequence was assembled with ampicillin resistance
163 and origin of replication cassettes into a high-copy plasmid, named "pGL-CPERlinker" (**Figure**
164 **1B**).

165 Using the newly optimized CPER workflow, infectious virus generated using as a
166 template a BAC construct encoding a GFP reporter SARS-CoV-2 [11] could be rescued as early
167 as day 3 post-transfection, as evidenced by the formation of GFP-positive syncytia (**Figure 1C**).
168 By day 5 post-transfection, massive cytopathic effects (CPE) could be observed. In comparison,
169 successful virus rescue using the 'classical' CPER approach was not observed until day 5 post-
170 transfection (**Figure 1C**), similar to previous reports [17, 18]. Therefore, the optimized CPER
171 workflow can accelerate SARS-CoV-2 rescue by at least 2 days.

172 **Cloning-free SARS-CoV-2 rescue and characterization of the CPER-derived recombinant**
173 **viruses**

bioRxiv preprint doi: https://doi.org/10.1101/2022.11.26.518005; this version posted November 30, 2022. The copyright holder for this preprint (which was not certified by peer review) is the author/funder, who has granted bioRxiv a license to display the preprint in perpetuity. It is made available under aCC-BY-NC-ND 4.0 International license.

174 We also applied the optimized CPER approach to rescue SARS-CoV-2 from purified
175 viral genomic RNA [17]. Adopting again the 10-fragment scheme reported by Torii *et al.* [18], we
176 successfully achieved specific amplification of all fragments from the first-strand cDNA that was
177 synthesized from purified viral genomic RNAs of three different virus strains, including the
178 ancestral strain WA1 and two VOCs (*i.e.* Beta and Omicron) (**Figure 2A**). We also performed
179 site-directed mutagenesis directly in the purified fragment #2 by overlap extension PCR using
180 the pair of primers for fragment #2 amplification (**Figure 2A**) and a pair of mutagenesis primers,
181 and could readily obtain the new mutant fragment #2 for all three viruses (**Figure 2B**).
182 Successful rescue of the WA1 and Beta viruses, as evidenced by CPE, was consistently
183 observed between day 3 and day 4, and the passage 0 (P0) stocks were typically harvested on
184 day 4 or day 5 when CPE was >90%. The use of Vero E6-TMPRSS2 cells ensured the integrity
185 of the furin cleavage site, as confirmed by sequencing of independently-rescued viruses (**Figure
186 2C**). The CPER-derived recombinant viruses also displayed the same plaque morphology as
187 their parental isolates (**Figure 2D**), and the P0 virus titers consistently reached ~10^6 PFU/mL
188 (**Figure 2E**).

189

190 **DISCUSSION**

191 CPER-based approaches offer considerable advantages over other reverse genetics
192 systems for engineering positive-strand recombinant viruses harboring large genomes of >10
193 kb. First, they are PCR-based and better preserve viral genome sequences than plasmids or
194 large DNA constructs (*i.e.* BACs) which require bacterial amplification. Second, CPER allows for
195 manipulation of viral genome sequences via flexible PCR strategies with high accuracy,
196 enabling rapid and reliable generation of recombinant mutant infectious clones for functional
197 analysis of viral genes and specific motifs.

bioRxiv preprint doi: https://doi.org/10.1101/2022.11.26.518005; this version posted November 30, 2022. The copyright holder for this preprint (which was not certified by peer review) is the author/funder, who has granted bioRxiv a license to display the preprint in perpetuity. It is made available under aCC-BY-NC-ND 4.0 International license.

198 The herein-reported optimized CPER system, which was developed as part of our
199 continuous efforts to define the role of SARS-CoV-2 genes in innate immune evasion (in
200 particular, Nsp3 and its PLpro de-ISGylation activity) ([26] and Gack lab, unpublished data),
201 addressed key limitations of the traditional CPER approaches that can compromise the
202 robustness and efficiency of SARS-CoV-2 rescue. We provided proof of concept that, with the
203 implementation of additional or modified steps – 5' end phosphorylation, nick sealing, direct
204 transfection into permissive cells – and through the use of a modified linker plasmid, SARS-
205 CoV-2 rescue can be accelerated. At this point, we have not yet systematically determined
206 which one(s) of these specific steps is functionally most important for the CPER optimization. It
207 is conceivable that the combination of the new practices leads to successful virus rescue in a
208 short time.

209 This optimized approach allowed for the accurate generation of reporter viruses and
210 recombinant VOC strains, which displayed similar replication capacities as their respective
211 parental viruses. The described optimization steps may be readily adapted also to other
212 positive-strand RNA viruses such as other coronaviruses or alphaviruses, flaviviruses, and
213 noroviruses. Further optimization of the reported workflow may be achieved by combining
214 CPER and nick ligation in one reaction and by using other permissive cells (*e.g.* Caco-2) for
215 transfection of the CPER product. Moreover, although the genome segmentation scheme and
216 primer sets used in our studies (previously reported by Torri *et al.*) conform to the genome
217 sequences of the selected Beta and Omicron strains, further optimization of the fragment
218 scheme and primer locations could be attempted, considering phylogenetic analysis of
219 sequence conservation, to achieve a universal set of primers that can be applied to all VOCs
220 and emerging viral strains. It is also important to deep-sequence CPER-derived recombinant
221 viruses and those generated by other reverse genetics systems, which would allow comparing
222 the overall fidelity of different virus rescue approaches.

bioRxiv preprint doi: https://doi.org/10.1101/2022.11.26.518005; this version posted November 30, 2022. The copyright holder for this preprint (which was not certified by peer review) is the author/funder, who has granted bioRxiv a license to display the preprint in perpetuity. It is made available under aCC-BY-NC-ND 4.0 International license.

223 Our optimized CPER method may promote the functional analysis of recombinant
224 viruses to evaluate viral determinants of pathogenesis, immune evasion and transmission. It
225 could also be useful for the efficient generation of replication-'crippled' viruses that may serve as
226 live-attenuated vaccines with potentially higher efficacy than currently available COVID-19
227 vaccines. The optimized CPER approach described herein may also facilitate the incorporation
228 of mechanism-based mutations that serve as built-in safety features (*e.g.* mutations in the Nsp1
229 gene and transcriptional regulatory sequence (TRS) [28, 29]) when studying certain viral
230 variants or mutants.

231

232 **Additional comments regarding ethics and biosafety.** Safe handling of viral agents such as
233 SARS-CoV-2 is of utmost importance. Work with SARS-CoV-2 including recombinant viruses
234 engineered using CPER (or other reverse genetics) approaches requires adequate biosafety
235 biocontainment and is subject to institutional, local and/or federal regulations. Considering the
236 ongoing debates about the dissemination of methods for reverse engineering of SARS-CoV-2
237 (see for example [30]), we consciously described in detail only the newly developed optimization
238 steps of the CPER method, while mostly referring to published reports for the other steps of the
239 CPER approach.

bioRxiv preprint doi: https://doi.org/10.1101/2022.11.26.518005; this version posted November 30, 2022. The copyright holder for this preprint (which was not certified by peer review) is the author/funder, who has granted bioRxiv a license to display the preprint in perpetuity. It is made available under aCC-BY-NC-ND 4.0 International license.

240 **MATERIALS AND METHODS**

241 **Biosafety**

242 SARS-CoV-2 genomic RNA extraction, cDNA synthesis, CPER transfection, and live
243 virus experiments were all conducted in the BSL-3 facility of the Cleveland Clinic Florida
244 Research and Innovation Center (CC-FRIC). Sterility-tested viral cDNA was handled in a BSL-2
245 laboratory following standard biosafety practices and procedures. All work was reviewed and
246 approved by the CC-FRIC Institutional Biosafety Committee in accordance with the National
247 Institutes of Health (NIH) Guidelines.

248 **Cells and viruses**

249 Vero E6 (#CRL-1586) and HEK293T (#CRL-3216) cells were purchased from the
250 American Type Culture Collection (ATCC) and were maintained in Dulbecco's modified Eagle's
251 medium (DMEM, Gibco) supplemented with 10% fetal bovine serum (FBS, Gibco), 2 mM L-
252 Glutamine (Gibco), 1 mM sodium pyruvate (Gibco) and 100 U/mL of penicillin–streptomycin
253 (Gibco). Vero E6 cells stably expressing human TMPRSS2 were generated by lentiviral
254 transduction followed by selection with blasticidin (40 µg/mL; Invivogen). SARS-CoV-2 strains
255 hCoV-19/USA-WA1/2020 (NR-52281), hCoV-19/USA/MD-HP01542/2021 (Lineage B.1.351;
256 Beta variant) (NR-55282), and hCoV-19/USA/MD-HP20874/2021 (Lineage B.1.1.529; Omicron
257 variant) (NR-56461) were obtained from BEI Resources, National Institute of Allergy and
258 Infectious Diseases (NIAID), NIH.

259 **Viral genomic RNA purification and first-strand cDNA synthesis**

260 Viral genomic RNA was purified from 280 µL virus-containing media using the QIAamp
261 Viral RNA Mini Kit (Qiagen) as per the manufacturer's instructions and eluted in 60 µL nuclease-
262 free water. Reverse transcription for first-strand cDNA synthesis was performed by using the
263 LunaScript RT SuperMix Kit (NEB) containing both oligo(dT) and random primers in a reaction

bioRxiv preprint doi: https://doi.org/10.1101/2022.11.26.518005; this version posted November 30, 2022. The copyright holder for this preprint (which was not certified by peer review) is the author/funder, who has granted bioRxiv a license to display the preprint in perpetuity. It is made available under aCC-BY-NC-ND 4.0 International license.

264 consisting of 10 μL genomic RNA, 4 μL 5× SuperMix and 6 μL nuclease-free water with the
265 cycling condition as follows: 2 min at 25°C, 20 min at 55°C, and 1 min at 95°C. One microliter of
266 RNase H (5 U; Thermo Scientific) was subsequently added and the reaction mix was incubated
267 at 37°C for 20 min.

268 **DNA constructs**

269 The bacterial artificial chromosome (BAC) encoding a GFP reporter SARS-CoV-2 in the
270 background of hCoV-19/Germany/BY-pBSCoV2-K49/2020 (GISAID EPI_ISL_2732373) was
271 kindly provided by Armin Ensser (Friedrich-Alexander University Erlangen-Nürnberg, Germany)
272 and has been described previously [11]. pGL-CPERlinker was assembled from synthetic DNA
273 oligonucleotides and fragments (IDT) as well as the ampicillin resistance cassette and the origin
274 of replication derived from pUC19 (NEB).

275 **CPER reaction and transfection**

276 To amplify the 10 viral cDNA fragments (either from BAC or the first-strand viral genomic
277 cDNA), previously reported primer sets were used [18]. The primers for amplification of the
278 linker fragment from pGL-CPERlinker are: GL-CPERlinkF (5'-
279 CTTAGGAGAATGACAAAAAAAAAAAAAAAAAAAAAAAAAAAGGCCGGCATGGTCCCAGCC-
280 3') and GL-CPERlinkR (5'-
281 GTTACCTGGGAAGGTATAAACCTTTAATACGGTTCACTAAACGAGCTCTGCTTATATAG-3').
282 Amplification of each fragment was carried out by using the PrimeSTAR Max DNA polymerase
283 (Takara Bio) in a 50 μL PCR reaction containing 0.2 μM each primer and 1 ng BAC or 2 μL viral
284 cDNA as the template with the cycling condition as follows: 10 s at 98°C; 35 cycles of 10 s at
285 98°C, 5 s at 55°C, 25 s at 72°C; and 2 min at 72°C. All PCR products were gel purified by using
286 the Monarch DNA Gel Extraction Kit (NEB) and eluted in 20 μL nuclease-free water. The
287 purified fragments were then 5' phosphorylated in a 50 μL reaction containing 10 U of T4

bioRxiv preprint doi: https://doi.org/10.1101/2022.11.26.518005; this version posted November 30, 2022. The copyright holder for this preprint (which was not certified by peer review) is the author/funder, who has granted bioRxiv a license to display the preprint in perpetuity. It is made available under aCC-BY-NC-ND 4.0 International license.

288 polynucleotide kinase (NEB) and cleaned up through the Monarch PCR & DNA Cleanup spin
289 columns (NEB). CPER assembly was performed as previously described by combining 0.05
290 pmol of each fragment in a 50 µL reaction containing 2.5 U PrimeSTAR GXL DNA polymerase
291 (Takara Bio) and using the 'condition 3' cycling parameters [18]. Immediately before
292 transfection, the CPER product was subject to post-PCR nick sealing for 30 min at 50°C and 30
293 min at 60°C in a 25 µL reaction containing 1 mM β-nicotinamide adenine dinucleotide (NAD+)
294 (NEB) and 0.5 µL HiFi Taq DNA ligase (NEB). The final CPER product was transfected into
295 Vero E6-TMPRSS2 cells seeded into 6-well plates (~ 5×10^5 cells per well) by using the
296 *Trans*IT-X2 Dynamic Delivery System (Mirus Bio) as per the manufacturer's instructions. After
297 24 hours, the culture media was replaced with DMEM containing 2% FBS, 2 mM L-Glutamine, 1
298 mM sodium pyruvate, 1× non-essential amino acids (Gibco), 10 mM HEPES (Gibco), and 100
299 U/mL of penicillin–streptomycin. For the classical CPER method, the unsealed CPER product
300 was first transfected into HEK293T cells by using *Trans*IT-LT1 (Mirus Bio), and the trypsinized
301 cells were then overlaid onto Vero E6-TMPRSS2 cells at 6 hours post-transfection, as
302 previously described [17].

303 **Virus titration and sequencing**

304 The titers of the P0 virus stocks were determined by plaque assay. Briefly, a monolayer-
305 culture system of Vero E6-TMPRSS2 cells was incubated with ten-fold serially diluted virus-
306 containing media. The inoculum was removed after 2 hours, and the cell monolayers were
307 washed twice with PBS and then overlaid with 1% colloidal microcrystalline cellulose (Sigma) in
308 MEM containing 2% FBS, 2 mM L-Glutamine, 1× non-essential amino acids, 10 mM HEPES,
309 and 100 U/mL of penicillin–streptomycin. Plaques were visualized by Coomassie Blue staining
310 on day 3. For P0 virus sequencing, viral genomic RNA was purified and the first-strand cDNA
311 was synthesized as described above. Nine fragments encompassing the whole genome [31]

bioRxiv preprint doi: https://doi.org/10.1101/2022.11.26.518005; this version posted November 30, 2022. The copyright holder for this preprint (which was not certified by peer review) is the author/funder, who has granted bioRxiv a license to display the preprint in perpetuity. It is made available under aCC-BY-NC-ND 4.0 International license.

312 were then amplified from the cDNA and subsequently subjected to Sanger (Azenta Life
313 Sciences) or Nanopore sequencing (Plasmidsaurus).

bioRxiv preprint doi: https://doi.org/10.1101/2022.11.26.518005; this version posted November 30, 2022. The copyright holder for this preprint (which was not certified by peer review) is the author/funder, who has granted bioRxiv a license to display the preprint in perpetuity. It is made available under aCC-BY-NC-ND 4.0 International license.

314 **AUTHOR CONTRIBUTIONS**

315 G.L. designed and performed all experiments and analyzed the data. M.U.G. supervised the
316 study. G.L. and M.U.G. wrote the manuscript.

317

318 **ACKNOWLEDGEMENTS**

319 This study was funded, in part, by the US National Institutes of Health grant R37 AI087846 (to
320 M.U.G.). We greatly thank Armin Ensser (Friedrich-Alexander University Erlangen-Nürnberg) for
321 providing reagents.

322

323 **DECLARATION OF INTERESTS**

324 The authors declare no competing interests.

bioRxiv preprint doi: https://doi.org/10.1101/2022.11.26.518005; this version posted November 30, 2022. The copyright holder for this preprint (which was not certified by peer review) is the author/funder, who has granted bioRxiv a license to display the preprint in perpetuity. It is made available under aCC-BY-NC-ND 4.0 International license.

325 **FIGURE LEGENDS**

326 **FIGURE 1. Generation of recombinant SARS-CoV-2 by using an optimized CPER**
327 **methodology.**

328 (**A**) Schematic of the optimized CPER system that includes new or modified steps including 5'
329 end phosphorylation, nick ligation, as well as direct transfection of permissive cells with the
330 CPER product. Specifically, the nine overlapping cDNA fragments (F1–F9/10) covering the full-
331 length SARS-CoV-2 genome were phosphorylated at the 5' end using T4 polynucleotide kinase
332 (PNK) before being subjected to CPER assembly using a modified linker fragment (as illustrated
333 in B). The circularized CPER product was then sealed at the staggered nicks by DNA ligation
334 using HiFi *Taq* DNA ligase, and the closed circular infectious cDNA clone was transfected into
335 Vero E6-TMPRSS2 cells for virus rescue. ‘P’ indicates phosphorylation.

336 (**B**) Map of the linker plasmid (pGL-CPERlinker) in which the hepatitis delta virus (HDV)
337 ribozyme, bovine growth hormone polyadenylation signal (bGH polyA), RNA polymerase II (Pol
338 II) transcription pause signal, and human cytomegalovirus (CMV) enhancer and promoter were
339 assembled together with the ampicillin resistance (AmpR) cassette and the origin of replication
340 (Ori) derived from the pUC19 plasmid (NEB).

341 (**C**) Comparison of the optimized CPER system with the original method as described by
342 Amarilla *et al.* [17] by rescuing a GFP reporter virus. GFP-positive syncytia were evident as
343 early as day 3 and day 5 post-transfection of the CPER product into Vero E6-TMPRSS2 cells,
344 respectively. Scale bar, 100 μm.

345

346 **FIGURE 2. Cloning-free generation and characterization of CPER-derived recombinant**
347 **SARS-CoV-2.**

bioRxiv preprint doi: https://doi.org/10.1101/2022.11.26.518005; this version posted November 30, 2022. The copyright holder for this preprint (which was not certified by peer review) is the author/funder, who has granted bioRxiv a license to display the preprint in perpetuity. It is made available under aCC-BY-NC-ND 4.0 International license.

348 (**A**) Representative gel images of the overlapping cDNA fragments amplified from purified
349 SARS-CoV-2 genomic RNAs of the indicated virus strains. The primer sets described by Torii *et*
350 *al.* [18] conform to the genome sequences of the ancestral strain (WA1) and the selected Beta
351 and Omicron variants of concern (VOCs) with 100% complementarity. MM, molecular marker.

352 (**B**) Schematic of the overlapping PCR strategy for site-directed mutagenesis in fragment 2 by
353 using purified PCR product as a template (top panel), as well as representative gel images of
354 the intermediate (2.1 and 2.2) and final (2^{mut}) PCR products (bottom panel). MM, molecular
355 marker.

356 (**C**) Sequencing confirmation of the integrity of the spike furin cleavage site of the passage 0
357 (P0) virus stocks from three independent virus rescues using the optimized CPER approach. aa,
358 amino acids; nt, nucleotides.

359 (**D**) Plaque morphology on Vero E6-TMPRSS2 cells of recombinant Beta (rBeta) generated by
360 optimized CPER as well as of its parental virus.

361 (**E**) Virus titers of the P0 stocks of CPER-derived recombinant WA1 (rWA1) and rBeta, collected
362 at day 5 and day 4 post-transfection of the CPER product, respectively (n = 4).

bioRxiv preprint doi: https://doi.org/10.1101/2022.11.26.518005; this version posted November 30, 2022. The copyright holder for this preprint (which was not certified by peer review) is the author/funder, who has granted bioRxiv a license to display the preprint in perpetuity. It is made available under aCC-BY-NC-ND 4.0 International license.

363 **REFERENCES**

364 1. Palese P, Zheng H, Engelhardt OG, Pleschka S, Garcia-Sastre A: **Negative-strand**
365 **RNA viruses: genetic engineering and applications.** *Proc Natl Acad Sci U S A* 1996,
366 **93:**11354-11358.
367 2. Aubry F, Nougairede A, Gould EA, de Lamballerie X: **Flavivirus reverse genetic**
368 **systems, construction techniques and applications: a historical perspective.**
369 *Antiviral Res* 2015, **114:**67-85.
370 3. Liu J, Liu Y, Xia H, Zou J, Weaver SC, Swanson KA, Cai H, Cutler M, Cooper D, Muik A,
371 et al: **BNT162b2-elicited neutralization of B.1.617 and other SARS-CoV-2 variants.**
372 *Nature* 2021, **596:**273-275.
373 4. Stobart CC, Moore ML: **RNA virus reverse genetics and vaccine design.** *Viruses*
374 2014, **6:**2531-2550.
375 5. Hu B, Guo H, Zhou P, Shi ZL: **Characteristics of SARS-CoV-2 and COVID-19.** *Nat*
376 *Rev Microbiol* 2021, **19:**141-154.
377 6. V'Kovski P, Kratzel A, Steiner S, Stalder H, Thiel V: **Coronavirus biology and**
378 **replication: implications for SARS-CoV-2.** *Nat Rev Microbiol* 2021, **19:**155-170.
379 7. Almazan F, Dediego ML, Galan C, Escors D, Alvarez E, Ortego J, Sola I, Zuniga S,
380 Alonso S, Moreno JL, et al: **Construction of a severe acute respiratory syndrome**
381 **coronavirus infectious cDNA clone and a replicon to study coronavirus RNA**
382 **synthesis.** *J Virol* 2006, **80:**10900-10906.
383 8. Yount B, Curtis KM, Fritz EA, Hensley LE, Jahrling PB, Prentice E, Denison MR,
384 Geisbert TW, Baric RS: **Reverse genetics with a full-length infectious cDNA of**
385 **severe acute respiratory syndrome coronavirus.** *Proc Natl Acad Sci U S A* 2003,
386 **100:**12995-13000.
387 9. Scobey T, Yount BL, Sims AC, Donaldson EF, Agnihothram SS, Menachery VD,
388 Graham RL, Swanstrom J, Bove PF, Kim JD, et al: **Reverse genetics with a full-length**
389 **infectious cDNA of the Middle East respiratory syndrome coronavirus.** *Proc Natl*
390 *Acad Sci U S A* 2013, **110:**16157-16162.
391 10. Terada Y, Kuroda Y, Morikawa S, Matsuura Y, Maeda K, Kamitani W: **Establishment of**
392 **a Virulent Full-Length cDNA Clone for Type I Feline Coronavirus Strain C3663.** *J*
393 *Virol* 2019, **93**.
394 11. Herrmann A, Jungnickl D, Cordsmeier A, Peter AS, Uberla K, Ensser A: **Cloning of a**
395 **Passage-Free SARS-CoV-2 Genome and Mutagenesis Using Red Recombination.**
396 *Int J Mol Sci* 2021, **22**.
397 12. Thi Nhu Thao T, Labroussaa F, Ebert N, V'Kovski P, Stalder H, Portmann J, Kelly J,
398 Steiner S, Holwerda M, Kratzel A, et al: **Rapid reconstruction of SARS-CoV-2 using a**
399 **synthetic genomics platform.** *Nature* 2020, **582:**561-565.
400 13. Xie X, Muruato A, Lokugamage KG, Narayanan K, Zhang X, Zou J, Liu J, Schindewolf
401 C, Bopp NE, Aguilar PV, et al: **An Infectious cDNA Clone of SARS-CoV-2.** *Cell Host*
402 *Microbe* 2020, **27:**841-848 e843.
403 14. Ye C, Chiem K, Park JG, Oladunni F, Platt RN, 2nd, Anderson T, Almazan F, de la Torre
404 JC, Martinez-Sobrido L: **Rescue of SARS-CoV-2 from a Single Bacterial Artificial**
405 **Chromosome.** *mBio* 2020, **11**.
406 15. Rihn SJ, Merits A, Bakshi S, Turnbull ML, Wickenhagen A, Alexander AJT, Baillie C,
407 Brennan B, Brown F, Brunker K, et al: **A plasmid DNA-launched SARS-CoV-2 reverse**
408 **genetics system and coronavirus toolkit for COVID-19 research.** *PLoS Biol* 2021,
409 **19:**e3001091.
410 16. Edmonds J, van Grinsven E, Prow N, Bosco-Lauth A, Brault AC, Bowen RA, Hall RA,
411 Khromykh AA: **A novel bacterium-free method for generation of flavivirus**

bioRxiv preprint doi: https://doi.org/10.1101/2022.11.26.518005; this version posted November 30, 2022. The copyright holder for this preprint (which was not certified by peer review) is the author/funder, who has granted bioRxiv a license to display the preprint in perpetuity. It is made available under aCC-BY-NC-ND 4.0 International license.

412 **infectious DNA by circular polymerase extension reaction allows accurate**
413 **recapitulation of viral heterogeneity.** *J Virol* 2013, **87:**2367-2372.
414 17. Amarilla AA, Sng JDJ, Parry R, Deerain JM, Potter JR, Setoh YX, Rawle DJ, Le TT,
415 Modhiran N, Wang X, et al: **A versatile reverse genetics platform for SARS-CoV-2**
416 **and other positive-strand RNA viruses.** *Nat Commun* 2021, **12:**3431.
417 18. Torii S, Ono C, Suzuki R, Morioka Y, Anzai I, Fauzyah Y, Maeda Y, Kamitani W,
418 Fukuhara T, Matsuura Y: **Establishment of a reverse genetics system for SARS-**
419 **CoV-2 using circular polymerase extension reaction.** *Cell Rep* 2021, **35:**109014.
420 19. Quan J, Tian J: **Circular polymerase extension cloning of complex gene libraries**
421 **and pathways.** *PLoS One* 2009, **4:**e6441.
422 20. Xia Y, Chu W, Qi Q, Xun L: **New insights into the QuikChange process guide the**
423 **use of Phusion DNA polymerase for site-directed mutagenesis.** *Nucleic Acids Res*
424 2015, **43:**e12.
425 21. Agapov A, Olina A, Kulbachinskiy A: **RNA polymerase pausing, stalling and bypass**
426 **during transcription of damaged DNA: from molecular basis to functional**
427 **consequences.** *Nucleic Acids Res* 2022, **50:**3018-3041.
428 22. Chu H, Chan JF, Yuen TT, Shuai H, Yuan S, Wang Y, Hu B, Yip CC, Tsang JO, Huang
429 X, et al: **Comparative tropism, replication kinetics, and cell damage profiling of**
430 **SARS-CoV-2 and SARS-CoV with implications for clinical manifestations,**
431 **transmissibility, and laboratory studies of COVID-19: an observational study.**
432 *Lancet Microbe* 2020, **1:**e14-e23.
433 23. Johnson BA, Xie X, Bailey AL, Kalveram B, Lokugamage KG, Muruato A, Zou J, Zhang
434 X, Juelich T, Smith JK, et al: **Loss of furin cleavage site attenuates SARS-CoV-2**
435 **pathogenesis.** *Nature* 2021, **591:**293-299.
436 24. Osada N, Kohara A, Yamaji T, Hirayama N, Kasai F, Sekizuka T, Kuroda M, Hanada K:
437 **The genome landscape of the african green monkey kidney-derived vero cell line.**
438 *DNA Res* 2014, **21:**673-683.
439 25. Shin D, Mukherjee R, Grewe D, Bojkova D, Baek K, Bhattacharya A, Schulz L, Widera
440 M, Mehdipour AR, Tascher G, et al: **Papain-like protease regulates SARS-CoV-2 viral**
441 **spread and innate immunity.** *Nature* 2020, **587:**657-662.
442 26. Liu G, Lee JH, Parker ZM, Acharya D, Chiang JJ, van Gent M, Riedl W, Davis-Gardner
443 ME, Wies E, Chiang C, Gack MU: **ISG15-dependent activation of the sensor MDA5 is**
444 **antagonized by the SARS-CoV-2 papain-like protease to evade host innate**
445 **immunity.** *Nat Microbiol* 2021, **6:**467-478.
446 27. Eggermont J, Proudfoot NJ: **Poly(A) signals and transcriptional pause sites combine**
447 **to prevent interference between RNA polymerase II promoters.** *EMBO J* 1993,
448 **12:**2539-2548.
449 28. Ricardo-Lax I, Luna JM, Thao TTN, Le Pen J, Yu Y, Hoffmann HH, Schneider WM,
450 Razooky BS, Fernandez-Martinez J, Schmidt F, et al: **Replication and single-cycle**
451 **delivery of SARS-CoV-2 replicons.** *Science* 2021, **374:**1099-1106.
452 29. Graham RL, Deming DJ, Deming ME, Yount BL, Baric RS: **Evaluation of a**
453 **recombination-resistant coronavirus as a broadly applicable, rapidly**
454 **implementable vaccine platform.** *Commun Biol* 2018, **1:**179.
455 30. Pannu J, Sandbrink JB, Watson M, Palmer MJ, Relman DA: **Protocols and risks: when**
456 **less is more.** *Nat Protoc* 2022, **17:**1-2.
457 31. Xie X, Lokugamage KG, Zhang X, Vu MN, Muruato AE, Menachery VD, Shi PY:
458 **Engineering SARS-CoV-2 using a reverse genetic system.** *Nat Protoc* 2021,
459 **16:**1761-1784.

460

A

SARS-CoV-2 genome

Orf1a

Orf1b

5' UTR

3' UTR

F1 F2 F3 F4 F5 F6 F7 F8 F9/10

5' End phosphorylation

CPER assembly

F1 F2 F3 F4 F5 F6 F7 F8 F9/10

Linker fragment

Nick ligation

Closed circular
infectious cDNA clone

Direct transfection
into Vero E6^{TMPRSS2}

Virus rescue

B

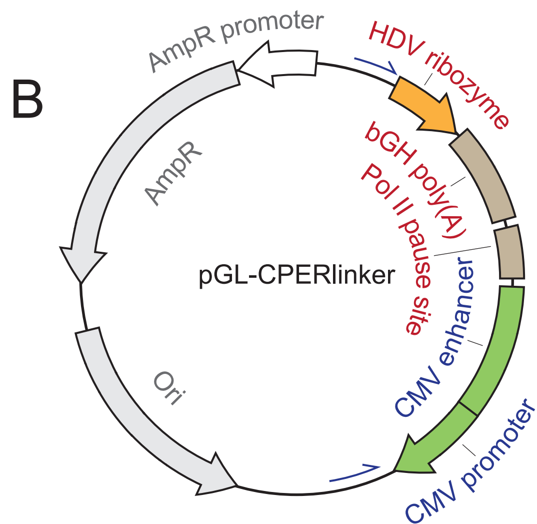

C

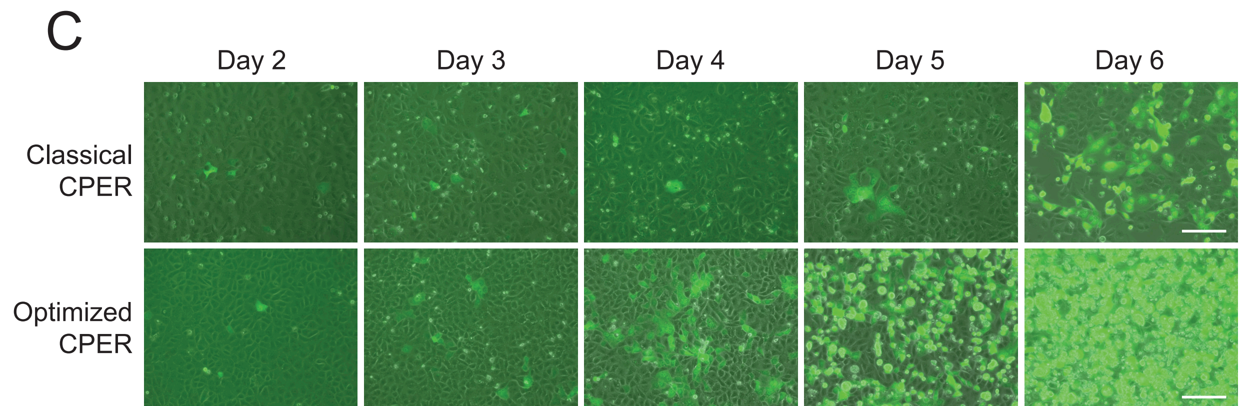

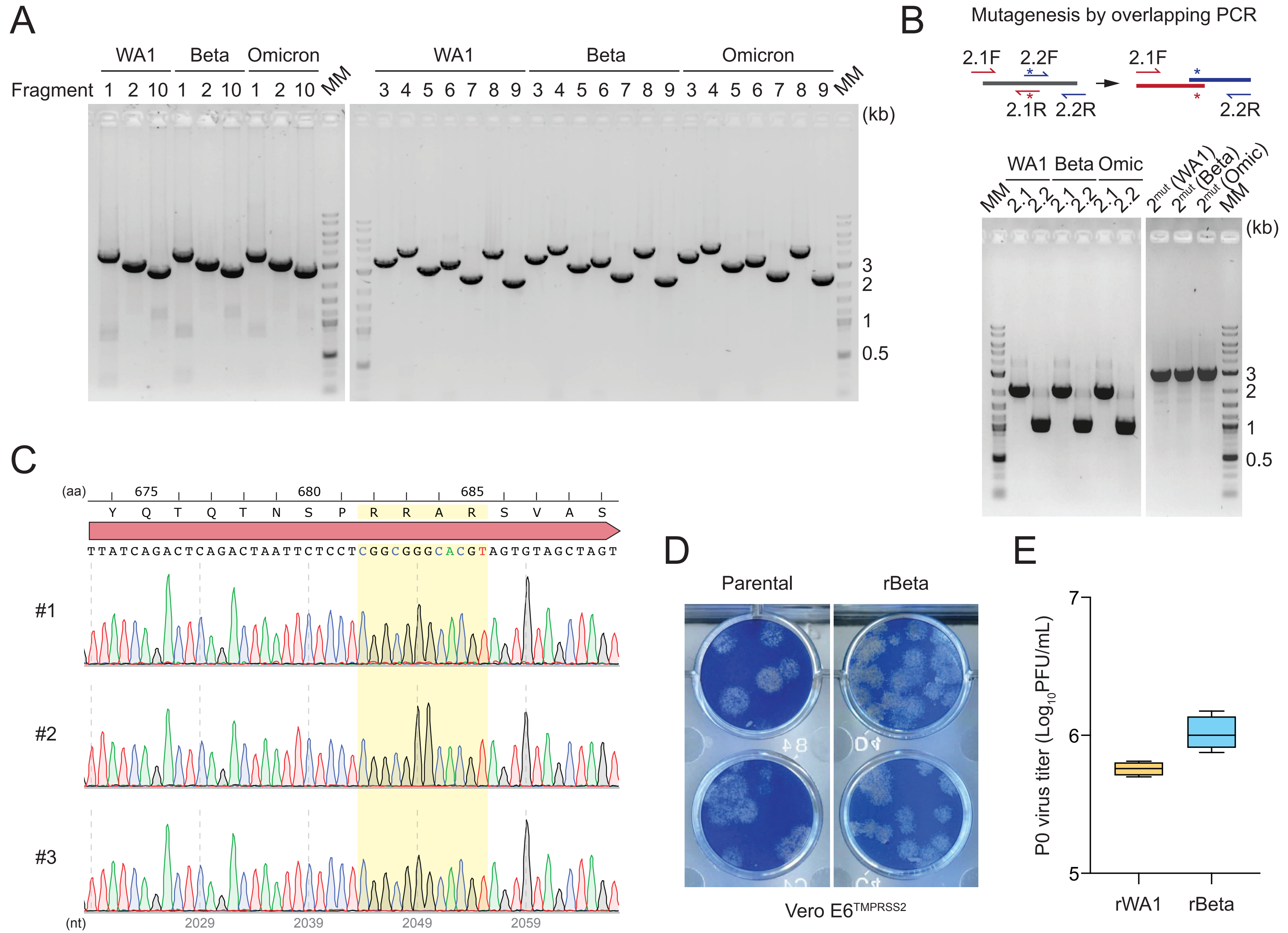
A
WA1
Beta
Omicron
Fragment 1 2 10 1 2 10 1 2 10 MM
3 4 5 6 7 8 9 3 4 5 6 7 8 9 3 4 5 6 7 8 9 MM
(kb)
3
2
1
0.5
B
Mutagenesis by overlapping PCR
2.1F
2.2F
2.1R
2.2R
WA1 Beta Omic
MM 2.1 2.2 2.1 2.2 2.1 2.2
2mut (WA1) 2mut (Beta) 2mut (Omic) MM
C
(aa)
675
680
685
Y Q T Q T N S P R R A R S V A S
TTATCAGACTCAGACTAATTCTCCTCGGCGGGCACGTAGTGTAGCTAGT
#1
#2
#3
(nt)
2029
2039
2049
2059
D
Parental
rBeta
Vero E6TMPRSS2
E
P0 virus titer (Log10PFU/mL)
7
6
5
rWA1
rBeta